OsteoArthritis and Cartilage (2005) **13,** 235–242

doi:10.1016/j.joca.2004.11.004

Osteoarthritis and Cartilage

International Cartilage Repair Society

OARSI OSTEOARTHRITIS RESEARCH SOCIETY INTERNATIONAL

Long-term periarticular bone adaptation in a feline knee injury model for post-traumatic experimental osteoarthritis

S. K. Boyd Ph.D.†‡§*, R. Müller Ph.D.‡, T. Leonard B.Sc.§ and W. Herzog Ph.D.§

† *Department of Mechanical and Manufacturing Engineering, University of Calgary, Calgary, Canada*

‡ *Institute for Biomedical Engineering, Swiss Federal Institute of Technology (ETH) and University of Zürich, Zürich, Switzerland*

§ *Human Performance Laboratory, Faculty of Kinesiology, University of Calgary, Calgary, Canada*

Summary

Objectives: This study investigates the long-term changes of the periarticular bone, including cancellous bone and the subchondral plate, in an anterior cruciate ligament (ACL)-transected cat for post-traumatic osteoarthritis (OA). These periarticular bone changes are related to the health of all knee tissues including articular cartilage degeneration and may be a key component of osteoarthritic development.

Methods: Thirteen cats (mean mass 4.9 $\pm$ 1.9 kg) were divided into three experimental groups: (1) normal controls, (2) 16 week, and (3) 5 year post unilateral ACL-transection (ACLT). Micro-computed tomography was used to scan the three-dimensional (3D) bone architecture of the proximal tibia, and analysis was performed on the subchondral plate and cancellous bone in the epiphyseal and metaphyseal regions of each bone.

Results: A decrease in cancellous bone mass (BV/TV) and subchondral plate thickness (Ct.Th) was observed 16 week post-ACLT, and the trend was statistically significant for the long-term animals (>5 year post-ACLT: BV/TV decreased 16.8%, $P < 0.003$; Ct.Th decreased 36.8%, $P < 0.03$). A decrease in bone mass was also observed as a function of animal age by comparing the young and aged normal control animals, however ACLT intensified those changes, particularly Ct.Th ($P < 0.009$) and anisotropy ($P < 0.045$). It was speculated that decreased internal joint loading despite normal kinematics may play an important role in the long-term reduction of cancellous bone volume and subchondral plate thinning.

Conclusions: The periarticular bone changes measured in this study were concurrent with articular cartilage degeneration, and suggest that bone may be a contributing factor in the aetiology of post-traumatic OA development.

Key words: Osteoarthritis, Post-traumatic injury, Micro-computed tomography, Feline, Knee.

Introduction

An acute injury to the knee, such as tearing of the anterior cruciate ligament (ACL), results in an increased likelihood of developing post-traumatic osteoarthritis (OA)[1,2]. Mechanical factors related to increased joint instability, such as altered loading and joint contact conditions, are often considered to play an important role in the aetiology of the disease. Of the tissues in the joint afflicted by the disease, degeneration of the articular cartilage is a clinical hallmark, and is of particular importance due to its critical role in normal joint function. However, there is strong interdependence of all tissues in the joint, and evidence of substantial periarticular bone changes in post-traumatic OA[3–5] suggest that bone may also be an important factor in the disease pathogenesis.

The architecture and strength of periarticular bone, including the subchondral plate (i.e., compact mineralized bone supporting the articular cartilage) and adjacent cancellous region, is sensitive to acute injury of the knee[6,7]. Using animal models to study OA by stimulating the pathological events leading to its development by ACL-transection (ACLT), it has been found that substantial changes to the periarticular bone can occur in the early stages following injury[8–10]. In a canine model, structural changes to the cancellous bone have been observed as early as 3 week post-ACLT, and a marked decrease of stiffness (−45%) and bone volume ratio (−35%) reported at 12 week post-ACLT, with no detectable change to subchondral plate thickness (Ct.Th)[11]. Based on long-term studies[12,13], it appears that the cancellous degradation persists at 54 month post-ACLT, and additionally the Ct.Th[13]. The early cancellous changes are likely caused by both mechanical (i.e., limb unloading)[14,15] and physiological factors (i.e., injury response)[16]. However, although the injury response, in terms of blood flow, has been shown to diminish after the first few months[16], unloading of the canine hind limb persists[14,15] and may be a dominating factor leading to the long-term periarticular changes.

In the feline ACLT model, in contrast to the canine model, the ground reaction forces (GRFs) and hind limb kinematics recover to near pre-surgical patterns within 5 month post-ACLT[17,18]. This recovery may be partially explained by

*Address correspondence and reprint requests to: Steven Boyd, Ph.D., Department of Mechanical and Manufacturing Engineering, University of Calgary, 2500 University Drive, N.W., Calgary, Alberta T2N 1N4, Canada. Tel: 1-403-220-4173; Fax: 1-403-282-8406; E-mail: skboyd@ucalgary.ca

Received 21 February 2004; revision accepted 7 November 2004.

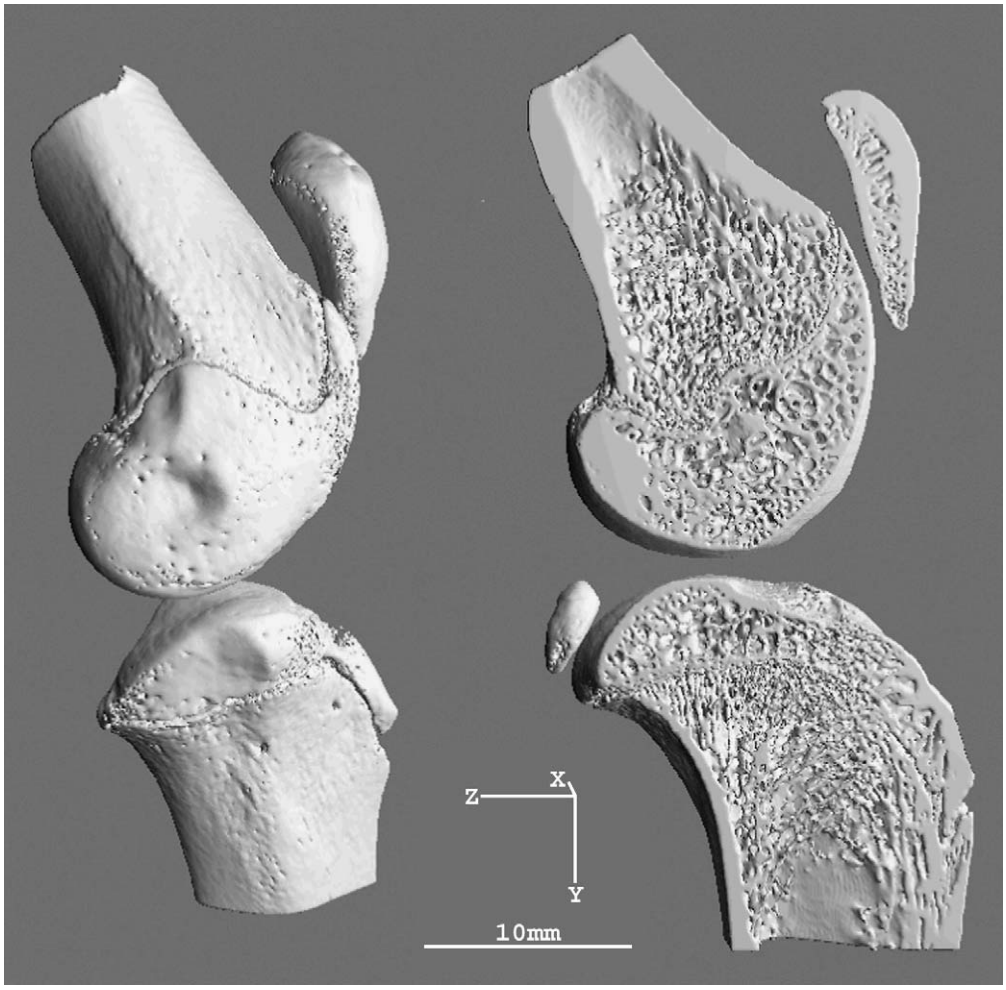

Fig. 1. The distal femur, patella and proximal tibia of a normal control cat knee scanned with micro-computed tomography (left), and a sagittal cut through the knee (right) exposing the internal bone structure.

differences in motor control patterns between species. However, despite the ability to recover, long-term studies of the feline model (i.e., >6 years) have found cartilage degradation and the formation of osteophytes at the joint margins consistent with the development of OA (Herzog *et al.*, unpublished data). Specifically, there is focal loss of articular cartilage on the medial tibial plateau, the femoral condyles and the retropatellar surface. Those areas where the cartilage is not completely eroded away show hypertrophic cartilage with surface lesions, and loss of proteoglycan in the superficial zone. The menisci appear fibrillated and exhibit 'bucket tears', particularly in the medial plateau. Synovial inflammation associated with ACLT returns to normal (qualitatively observed) approximately 1 month post-ACLT. Although gait patterns, loading and cartilage properties are well understood in long-term studies of this model of OA[19], the implications of these degenerations on the long-term bone changes are not known.

The present study was aimed at quantifying the changes to the periarticular bone in a long-term feline model of post-traumatic OA. It was hypothesized that despite the return to near normal gait patterns, as measured by GRFs and kinematics, the periarticular bone architecture (cancellous bone and subchondral plate) would not recover to normal values in the long term, and the bone degradation would coincide with the degradation of other joint tissues such as the articular cartilage.

Methods

A total of 13 cats were used (mean mass 4.9 ± 1.9 kg) that were part of a larger research project aimed at investigating the long-term development of post-traumatic OA. The cats were divided into three main groups: (1) normal controls ($n = 4$), (2) early post-ACLT (16 weeks, $n = 4$), and (3) long-term post-ACLT (60 to 74 months, $n = 5$, mean age 67 ± 6 months). The transection was performed unilaterally (left hind limb) using an established protocol[20]. The normal controls were subdivided into two small groups consisting of two young adult animals (2 year old) and two old adult animals (18 and 22 year old) to provide baseline bone architecture as a function of natural aging. The study was approved by The University of Calgary Animal Care Committee.

MICRO-TOMOGRAPHIC SCANNING

At death, the tibiae were cleaned of all soft tissues and stored ($-80\,^{\circ}$C) in saline-soaked gauze. The proximal 6 cm

of the tibiae were cut mid-shaft, and this entire portion of the bone was placed in the micro-tomographic scanner (μCT 40, Scanco Medical, Bassersdorf, Switzerland) for measurement. The proximal 16 mm were scanned at a nominal resolution of 30 μm (isotropic voxel dimension), and a constrained Gaussian filter ($\sigma = 1.2$, finite support of 1) was used to suppress noise in the original volume data. Global thresholding (224‰ of maximal image value) was applied to extract the mineralized bone phase[21]. Qualitative comparisons of the bone architecture were made through three-dimensional (3D) visualizations of the image data using an extended Marching Cubes algorithm[22,23]. One scan of an intact normal cat knee, including the distal femur, patella and proximal tibia, was performed to provide an overview of the feline knee joint (Fig. 1).

QUANTITATIVE ANALYSIS

The regions for analysis were segmented from the 3D images of the tibia using a semi-automated contouring tool (Scanco Medical). The subchondral plate and neighboring cortical bone were extracted from the images (no explicit distinction was made between compact mineralized bone and calcified cartilage due to the thresholding technique used to extract the bone phase), and the cancellous bone was divided into two main parts defined by the growth plate: the epiphyseal and metaphyseal cancellous regions (Fig. 2).

The morphological measures made on the cancellous bone included 3D metrics such as bone volume density (BV/TV), bone surface density (BS/TV), trabecular thickness (Tb.Th), separation (Tb.Sp) and number (Tb.N)[24,25]. Also, 3D non-metric measures included connectivity density (Conn.D)[26] which provides a measure of the number of connections per unit volume, and the degree of material anisotropy (DA) which provides information about the distribution of bone[27]. Thickness of the subchondral plate (Ct.Th) was assessed in the medial and lateral tibial plateaus in the central weight bearing region by averaging multiple measurement samples (three per side) in extracted 2D cross-sections of those regions.

STATISTICAL ANALYSIS

Statistical tests (SPSS, Chicago, IL, USA) for morphological parameters included a two-way analysis of variance

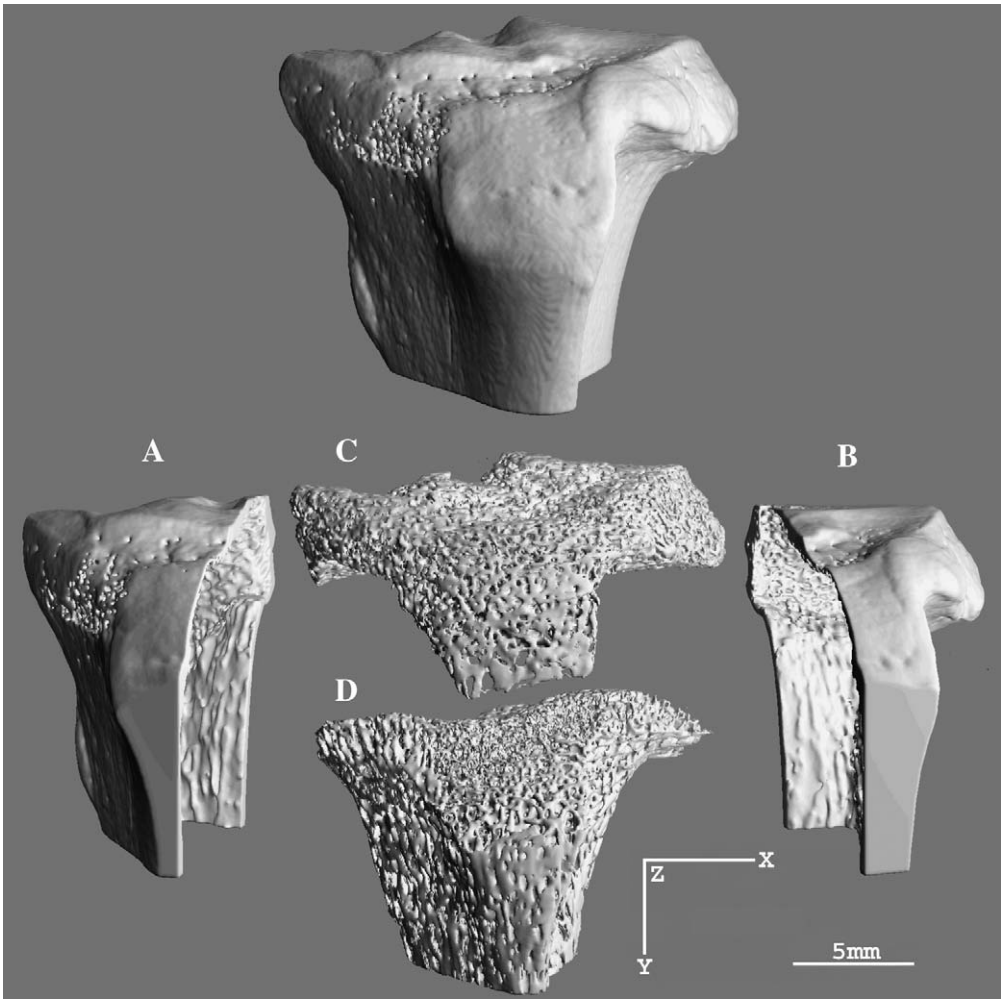

Fig. 2. Each three-dimensional image of the proximal tibia (top) was segmented into three distinct regions (bottom) by semi-automated contouring: the subchondral bone plate on the medial (A) and lateral (B) articular surface, and epiphyseal (C) and metaphyseal (D) cancellous bone located above and below the epiphyseal plate (the epiphyseal plate was distinguishable in the micro-CT images for animals of all ages). Morphological analyses were performed on these regions separately.

(ANOVA; $P < 0.05$) with one factor being time post-operation (0, 16 weeks, >60 months) and the other being operation (ACLT vs contralateral). A Bonferroni adjustment for multiple comparisons was used when identifying significant morphological changes. Subsequently, a *post hoc* analysis using a paired *t*-test identified intra-animal differences (ACLT vs contralateral) for the morphological parameters at 16 weeks and long-term post-ACLT. The normal controls provided a qualitative baseline comparison, but due to limited group size, these data are presented descriptively.

Results

Bone micro-architectural changes of the operated limbs compared to the contralateral controls were evident in both experimental groups, as well as changes in the normal controls (old vs young). Three-dimensional visualizations, showing sagittal plane cross-sections of representative samples from each experimental group, illustrate the 3D micro-architecture qualitatively (Fig. 3), and one 3D visualization of a typical normal control (as part of the entire knee joint) can be used for comparison with those of operated animals (Fig. 1).

In the early experimental group (16 week post-ACLT), intra-animal quantitative differences in the morphological properties measured were evident, however only measured decreases of anisotropy and Ct.Th were statistically significant. In the long-term experimental group (i.e., >60 month post-ACLT), the intra-animal morphological changes were more pronounced, and all were statistically significant with the exception of the Tb.N. The morphological measures from all groups (normals, young and long-term experimental animals) are presented for the epiphyseal cancellous region (Fig. 4). The general trend of morphological changes in the cancellous bone was a decrease in bone volume ratio (BV/TV) and Tb.Th coinciding with increased Tb.Sp and bone surface area (BS/BV). Analyses for the cancellous region below the epiphyseal plate had the same trends for these morphological measures, though the magnitudes of the changes were less pronounced (data not presented).

Based on the two-way ANOVA, the ACLT operation resulted in a significant decrease of Ct.Th ($P < 0.009$) and anisotropy ($P < 0.045$) over the experimental time frame (Fig. 4). Additionally, the only morphological parameter significantly affected by the factor of time post-operation was Ct.Th ($P < 0.031$).

Ct.Th changes were clearly evident in all groups, with substantially decreased thickness in the ACLT knee of the long-term animals. Thinning of the subchondral plate occurred as a function of age. However, the degree of thinning was exacerbated by the ACLT procedure, resulting in up to a 50% decrease compared to the normal control animals (Fig. 5).

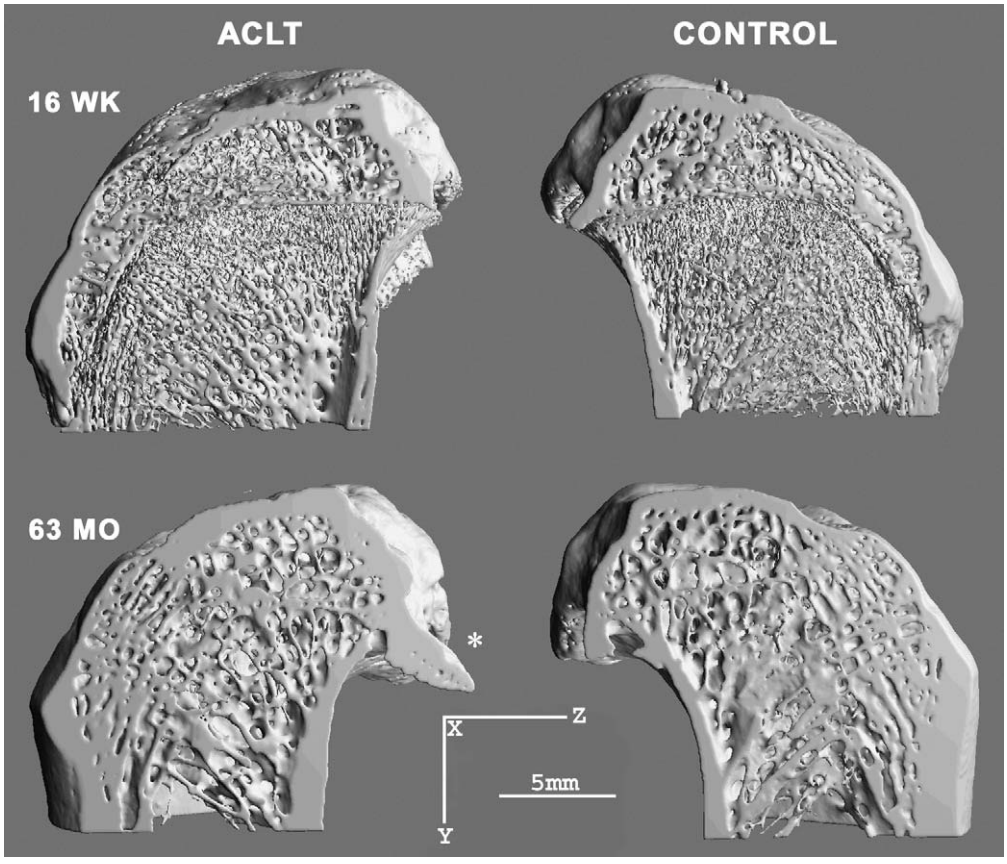

Fig. 3. Sample sagittal cross-sections through the proximal tibia of a 16 week post-ACLT (top) and 63 month post-ACLT (bottom) cat. For each sample, the ACLT knee (left) and contralateral control (right) is presented for comparison. In addition to the morphological changes which are quantified in Fig. 4, the formation of an osteophyte (*) can be observed in the long-term ACLT limb.

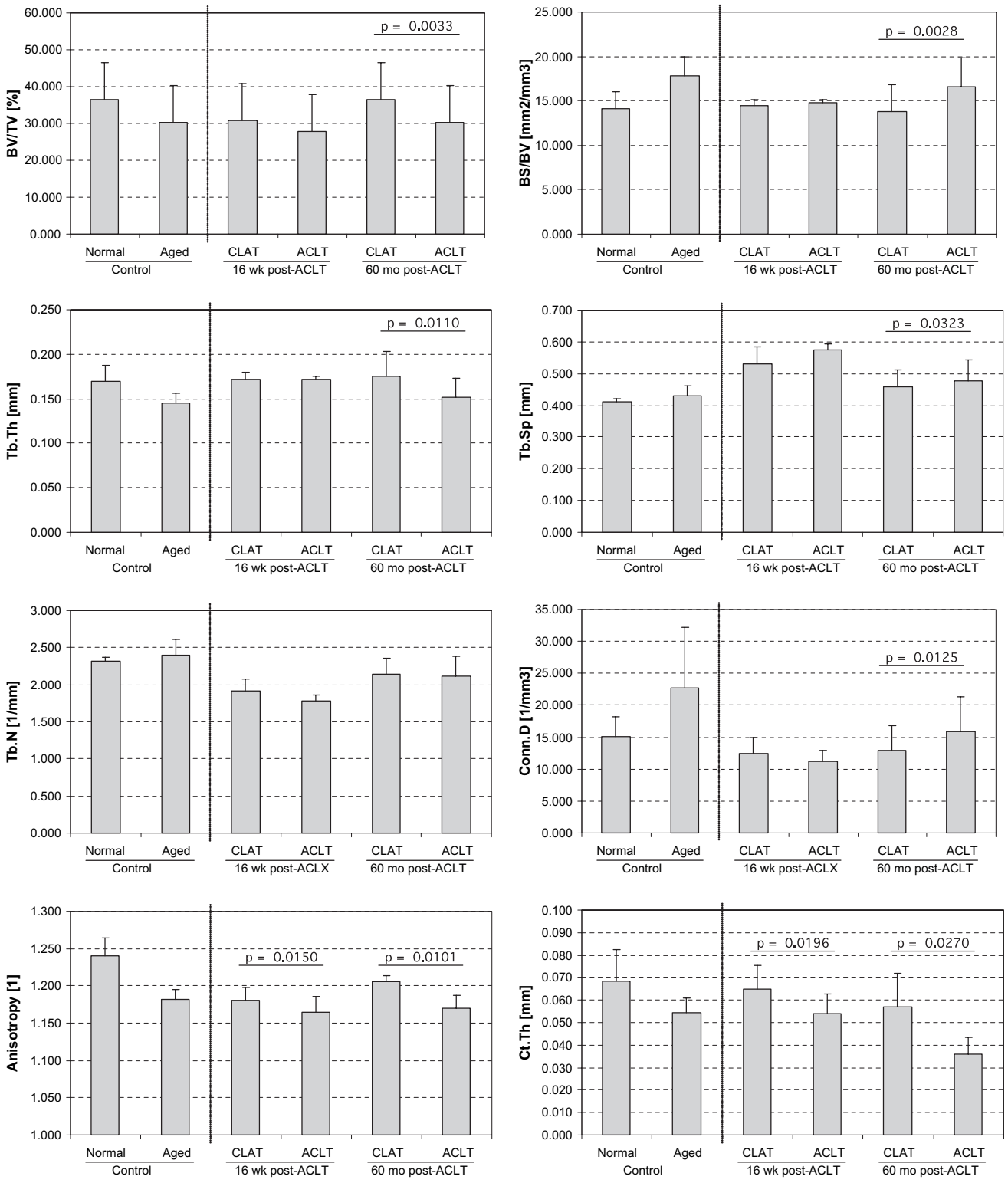

Fig. 4. Morphological measurements for the cancellous bone located proximal to the epiphyseal plate. Each plot contains mean and standard deviation error bars. Pair-wise *t*-tests were performed for the 16 week and 60 month experimental groups (statistical significance indicated for $P < 0.05$), and the normal and aged control groups are presented descriptively. ACLT refers to the operated limb and CLAT refers to the contralateral limb. The measured parameters include bone volume ratio (BV/TV), bone surface area (BS/BV), trabecular thickness (Tb.Th), trabecular separation (Tb.Sp), trabecular number (Tb.N), connectivity density (Conn.D), anisotropy and subchondral plate thickness (Ct.Th).

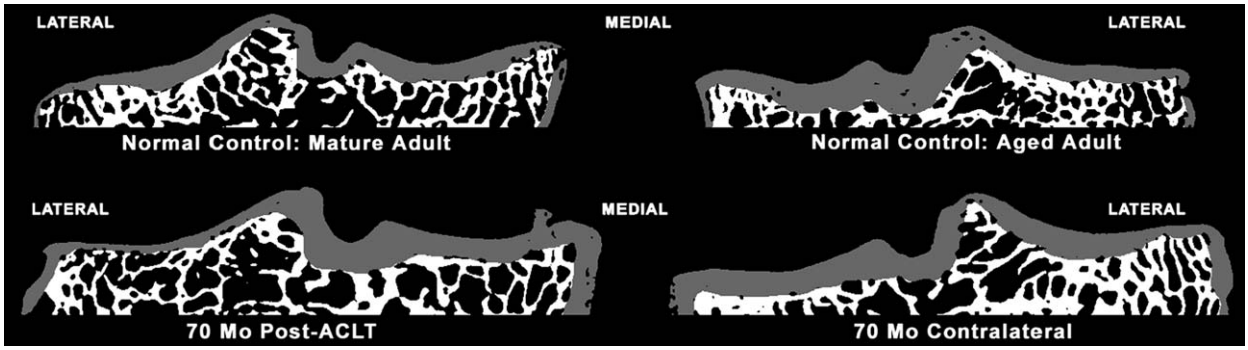

Fig. 5. Comparison of the subchondral plate (shaded gray) and periarticular cancellous bone (shaded white) from the normal control (top) and the long-term ACLT group (bottom). Samples from the normal control include a skeletally mature adult (left) and an aged adult (right). The operated and control limb of the ACLT animal is shown below (70 month post-ACLT). The lateral compartment of the joint following long-term ACLT is extremely thinned, and an osteophyte can be observed in the medial compartment.

Discussion

Transection of the ACL has been shown to lead to dramatic early changes in the periarticular bone structure of the ACL-transected dog model[8,9], which are evident in long-term follow-up of the canine model[12,13]. Although long-term studies in the ACL-transected cat have demonstrated degradation of the articular cartilage and development of osteophytes[19], the changes to the periarticular bone have remained unknown. The purpose of this study was to investigate the long-term changes to the periarticular bone in the cat model, which despite the return to normal external loading in the operated limb, still develops OA signs long term. It is clear from the results presented here that, concurrent to the articular cartilage degeneration, changes to the subchondral plate and cancellous bone occur as early as 16 week post-ACLT, and these changes become more pronounced in the long-term development of the disease.

Changes to the periarticular bone following ACLT are not attributable solely to disuse following the operation, and is likely an integral part of the aetiology of post-traumatic (secondary) OA that is concurrent with cartilage degradation. In the canine model, the reduced limb loading based on GRF measurements[14,15,28] plays a confounding role in the dramatic loss of bone that occurs[8,9], but because GRFs do not fully recover in the dog model the extent of this effect has been unclear. However, in this ACL-transected cat model, the GRFs return to near normal levels by 16−18 week post-ACLT[18] and still, in this model, signs of OA developed, including changes to the periarticular cancellous bone and subchondral plate. The results from these two animal models suggest that, although altered loading likely plays an important role in the long-term bone adaptations and short-term disuse and synovial inflammation are probably important early factors, the long-term bone changes cannot be explained solely by these transitory effects. However, altered forces in the periarticular bone can also occur due to changes in the *internal* knee contact[17,29] that happens as a result of the loss of ACL integrity. In the ACL-transected cat model, it has been shown that at 16 week post-ACLT, peak internal contact forces are reduced and contact areas are increased in the ACL-transected knees compared to the contralateral limbs[17,30], which suggests an average decrease in contact pressure. Therefore, while the early unloading and inflammation may result in an early transitory effect, the long-term bone loss reported here cannot be explained by those factors alone, and may be a result of decreased internal contact pressures as a result of the loss of the ACL.

Periarticular bone changes in the ACL-transected cat model followed similar patterns to the canine model[11−13]. Although the early loss of periarticular bone was less dramatic, this may be due to a difference in the motor control of the two animal models, or due to the young age of the 16 week post-ACLT group. In the young ACLT group, the epiphyseal plate was more evident than in the long-term experimental group, and the normal controls. (These animals were not part of the original long-term study, and although they had reached maturity at the time of ACLT procedure, i.e., >1 year old, skeletal maturity in terms of closure of the epiphyseal plate was not complete.) The early dramatic loss of cancellous bone in the canine model indicated that adaptation occurs in two-phases: early loss (i.e., immediately after 'early' initial trauma), followed by sustained changes. In the cat model, however, bone adaptation appears to be a more gradual process. Nonetheless, the decrease in periarticular bone is consistent with observations in patients with ACL-deficiency[31,32], and patients with idiopathic (primary) OA[33].

Additionally, cartilage erosion and osteophyte formation observed in the long-term animals was consistent with the development of OA observed clinically.

In contrast to the thickened subchondral plate reported in the canine[12] and guinea pig models[34,35], the subchondral plate was significantly thinner in both the medial and lateral compartments in this long-term feline model. The basis for the difference in subchondral bone pathology among these models is unclear, however a possible factor may be differences in motor control that affects external kinematics and internal contact forces. The hind limb kinematics of the feline model return to near baseline values within 5 month post-ACLT which differs from the canine model which has sustained altered hind limb kinematics (guinea pig kinematics are not well known). Another important factor may be the difference in pathogenesis between primary OA and secondary OA. The guinea pig is a model of spontaneous OA[36] (i.e., primary OA) that can be accelerated by menisectomy[34,35], whereas the feline model is purely a post-traumatic injury model (i.e., secondary OA). Despite the fact that cartilage erosion is reported in both the guinea pig and feline OA models, it is possible that the pathogenesis of OA affecting subchondral bone differs in primary and secondary OA.

The possibility to study long-term changes in an experimental model of OA is extremely rare, hence the small number of animals in each experimental group. Contralateral limbs provide controls, however changes to these joints may be influenced by the ACLT via compensatory mechanisms. Nevertheless, a contralateral limb provides a good internal comparison, and may best reflect a unilateral injury common in human patients. The normal control animals in this study also provide a basis of comparison, and were divided into normal (i.e., <3 year old) and aged (i.e., >18 year old) animals. It should be cautioned, however, that the aged controls were much older than the long-term ACLT animals (<10 year old vs >18 year old, respectively). Nevertheless, the two normal control groups emphasize that bone loss occurs with age, but that the ACLT procedure augments those morphological changes, in particular, loss of Ct.Th. Given that the only morphological change that was *not* significant in the long-term animals was Tb.N, this suggests that bone loss occurs primarily through thinning of the cancellous structure with minimal loss of trabecular bridges.

In conclusion, this study presents the long-term changes to periarticular bone that occur at least as early as the first signs of cartilage degradation (i.e., swelling), and suggests adaptation of bone as an important component in the aetiology of post-traumatic OA.

Acknowledgments

This study was funded by the Canadian Institutes of Health Research (CIHR), Swiss National Science Foundation (FP 620-58097.99), Natural Sciences and Engineering Research Council (NSERC) of Canada, and Alberta Heritage Foundation for Medical Research (AHFMR).

References

1. Noyes FR, Mooar PA, Matthews DS, Butler DL. The symptomatic anterior cruciate-deficient knee. Part I: The long-term functional stability in athletically active individuals. J Bone Joint Surg 1983;65-A:154–62.
2. Roos H, Adalberth T, Dahlberg L, Lohmander LS. Osteoarthritis of the knee after injury to the anterior cruciate ligament or meniscus: the influence of time and age. Osteoarthritis Cartilage 1995;3(4):261–7.
3. Radin EL, Martin RB, Burr DB, Caterson B, Boyd RD, Goodwin C. Effects of mechanical loading on the tissues of the rabbit knee. J Orthop Res 1984;2(3): 221–34.
4. Radin EL, Rose RM. Role of subchondral bone in the initiation and progression of cartilage damage. Clin Orthop 1986;213:34–40.
5. Brown TD, Radin EL, Martin RB, Burr DB. Finite element studies of some juxtarticular stress changes due to localized subchondral stiffening. J Biomech 1984;17(1):11–24.
6. Burr DB, Schaffler MB. The involvement of subchondral mineralized tissues in osteoarthrosis: quantitative microscopic evidence. Microsc Res Tech 1997;37(4): 343–57.
7. Bailey AJ, Mansell JP. Do subchondral bone changes exacerbate or precede articular cartilage destruction in osteoarthritis of the elderly? Gerontology 1997;43(5): 296–304.
8. Dedrick DK, Goulet RW, Huston L, Goldstein SA, Bole GG. Early bone changes in experimental osteoarthritis using microscopic computed tomography. J Rheumatol 1991;27(Suppl):44–5.
9. Boyd SK, Müller R, Matyas JR, Wohl GR, Zernicke RF. Early morphometric and anisotropic change in periarticular cancellous bone in a model of experimental knee osteoarthritis quantified using microcomputed tomography. Clin Biomech (Bristol, Avon) 2000;15(8): 624–31.
10. Gilbertson EM. Development of periarticular osteophytes in experimentally induced osteoarthritis in the dog. A study using microradiographic, microangiographic, and fluorescent bone-labelling techniques. Ann Rheum Dis 1975;34(1):12–25.
11. Boyd SK, Müller R, Zernicke RF. Mechanical and architectural bone adaptation in early stage experimental osteoarthritis. J Bone Miner Res 2002;17(4): 687–94.
12. Brandt KD, Myers SL, Burr D, Albrecht M. Osteoarthritic changes in canine articular cartilage, subchondral bone, and synovium fifty-four months after transection of the anterior cruciate ligament. Arthritis Rheum 1991; 34(12):1560–70.
13. Dedrick DK, Goldstein SA, Brandt KD, O'Connor BL, Goulet RW, Albrecht M. A longitudinal study of subchondral plate and trabecular bone in cruciate-deficient dogs with osteoarthritis followed up for 54 months. Arthritis Rheum 1993;36(10):1460–7.
14. Korvick DL, Pijanowski GJ, Schaeffer DJ. Three-dimensional kinematics of the intact and cranial cruciate ligament-deficient stifle of dogs. J Biomech 1994;27(1):77–87.
15. O'Connor BL, Visco DM, Heck DA, Myers SL, Brandt KD. Gait alterations in dogs after transection of the anterior cruciate ligament. Arthritis Rheum 1989;32(9): 1142–7.
16. Bray RC, Butterwick DJ, Doschak MR, Tyberg JV. Coloured microsphere assessment of blood flow to knee ligaments in adult rabbits: effects of injury. J Orthop Res 1996;14(4):618–25.
17. Herzog W, Diet S, Suter E, Mayzus P, Leonard TR, Müller C, *et al*. Material and functional properties of articular cartilage and patellofemoral contact mechanics in an experimental model of osteoarthritis. J Biomech 1998;31:1137–45.
18. Herzog W, Hasler EM, Maitland ME, Suter E, Leonard TR, Müller C. *In-vivo* mechanics and *in-situ* stability of the anterior cruciate ligament-deficient knee—an animal model of osteoporosis. Outl Biomech Res 1999;1:11–27.
19. Suter E, Herzog W, Leonard TR, Nguyen H. One-year changes in hind limb kinematics, ground reaction forces and knee stability in an experimental model of osteoarthritis. J Biomech 1998;31:511–7.
20. Herzog W, Adams ME, Matyas JR, Brooks JG. Hindlimb loading, morphology and biochemistry of articular cartilage in the ACL-deficient cat knee. Osteoarthritis Cartilage 1993;1:243–51.
21. Rüegsegger P, Koller B, Müller R. A microtomographic system for the nondestructive evaluation of bone architecture. Calcif Tissue Int 1996;58(1):24–9.
22. Lorensen WE, Cline HE. Marching cubes: a high resolution 3D surface construction algorithm. Comput Graph 1987;21(4):163–9.
23. Müller R, Hildebrand T, Rüegsegger P. Non-invasive bone biopsy: a new method to analyse and display the

three-dimensional structure of trabecular bone. Phys Med Biol 1994;39(1):145–64.
24. Hildebrand T, Rüegsegger P. A new method for the model-independent assessment of thickness in three-dimensional images. J Microsc 1997;185(1): 67–75.
25. Hildebrand T, Laib A, Müller R, Dequeker J, Rüegsegger P. Direct three-dimensional morphometric analysis of human cancellous bone: microstructural data from spine, femur, iliac crest, and calcaneus. J Bone Miner Res 1999;14(7):1167–74.
26. Odgaard A, Gundersen HJ. Quantification of connectivity in cancellous bone, with special emphasis on 3-D reconstructions. Bone 1993;14(2):173–82.
27. Laib A, Barou O, Vico L, Lafage-Proust MH, Alexandre C, Rüegsegger P. 3D micro-computed tomography of trabecular and cortical bone architecture with application to a rat model of immobilisation osteoporosis. Med Biol Eng Comput 2000;38:326–32.
28. Vilensky JA, O'Connor BL, Brandt KD, Dunn EA, Rogers PI, DeLong CA. Serial kinematic analysis of the unstable knee after transection of the anterior cruciate ligament: temporal and angular changes in a canine model of osteoarthritis. J Orthop Res 1994; 12(2):229–37.
29. Boyd SK, Ronsky JL. Normal and ACL-deficient *in-situ* measurement of patellofemoral joint contact. J Appl Biomech 2000;16:111–23.
30. Hasler EM, Herzog W, Leonard TR, Stano A, Nguyen H. *In vivo* knee joint loading and kinematics before and after ACL transection in an animal model. J Biomech 1998;31(3):253–62.
31. Leppälä J, Kannus P, Natri A, Pasanen M, Sievänen H, Vuori I, *et al*. Effect of anterior cruciate ligament injury of the knee on bone mineral density of the spine and affected lower extremity: a prospective one-year follow-up study. Calcif Tissue Int 1999;64(4):357–63.
32. Kannus P, Sievänen H, Järvinen M, Heinonen A, Oja P, Vuori I. A cruciate ligament injury produces considerable, permanent osteoporosis in the affected knee. J Bone Miner Res 1992;7(12):1429–34.
33. Day JS, Ding M, van der Linden JC, Hvid I, Sumner DR, Weinans H. A decreased subchondral trabecular bone tissue elastic modulus is associated with per-arthritic cartilage damage. J Orthop Res 2001;19:914–8.
34. Pastoureau P, Leduc S, Chomel A, De Ceuninck F. Quantitative assessment of articular cartilage and subchondral bone histology in the meniscectomized guinea pig model of osteoarthritis. Osteoarthritis Cartilage 2003;11(6):412–23.
35. Pastoureau PC, Chomel AC, Bonnet J. Evidence of early subchondral bone changes in the meniscectomized guinea pig. A densitometric study using dual-energy X-ray absorptiometry subregional analysis. Osteoarthritis Cartilage 1999;7(5):466–73.
36. Tessier JJ, Bowyer J, Brownrigg NJ, Peers IS, Westwood FR, Waterton JC, *et al*. Characterisation of the guinea pig model of osteoarthritis by *in vivo* three-dimensional magnetic resonance imaging. Osteoarthritis Cartilage 2003;11(12):845–53.